

Real-time and quantitative monitoring of CO₂ injection with rapid-repeat time-lapse vertical seismic profile data

Xiaohui Cai¹, Kristopher. Innanen¹, Qi Hu¹, Scott Keating², Matthew Eaid³, and Donald Lawton⁴

¹ Dept. of Geoscience, CREWES Project, University of Calgary, Calgary, Canada

² ETH, Zurich, Switzerland

³ Chevron, Houston, Texas, USA

⁴ Containment and Monitoring Institute, Carbon Management Canada, Calgary, Canada

Summary

In recent years our research group has observed quasi-transient changes in seismic transmission data associated with CO₂ injection (Innanen et al., 2019). Here, we present images generated through elastic full waveform inversion (EFWI) of rapid-repeat time-lapse vertical seismic profile (VSP) field data, acquired with a fixed source shooting across an injection plume at roughly 15-minute intervals over several days. These images, achieved by the combined distributed acoustic sensing (DAS) and geophone data, represent snapshots of clear transient changes in the vicinity of the injection well. The field data inversion images demonstrate the combined sparse-space geophone and DAS VSP can be new and informative monitoring modes.

Introduction

CO₂ monitoring ensures the effectiveness of geological storage after CO₂ is injected into the ground and prevents environmental hazards caused by possible CO₂ leakage. Time-lapse VSP surveys are likely to be a key technology for monitoring CO₂ injection and verifying containment and storage. Practical and low-cost measurement, monitoring, and validation are significant gaps in technology for large-scale implementation of carbon storage.

Full waveform inversion (FWI) is now regularly used for quantitative assessing images of structures under complex geological conditions (Pratt, 2004; Virieux and Operto, 2009; Pan et al., 2019; Keating and Innanen, 2019; Eaid et al., 2020; Hu et al., 2023), and it makes use of the waveform information, gradually approximating plausible high-resolution models by matching field and simulation data. There are several published examples of successful FWI applications to VSP (Charara et al., 1996; Owusu et al., 2016), and VSP-FWI applications for seismic monitoring (Egorov et al., 2017). However, there are very few cases of FWI based on rapid-repeat time-lapse VSP data for real-time and quantitative seismic monitoring.

DAS is a technology that enables the recording of seismic data using fiber-optic cables instead of traditional sensors (Daley et al., 2016; Spikes, 2019). DAS is suitable for acquiring VSP surveys for its high sensitivity to the direction parallel to the fiber. This report represents field results pointing towards methods for characterizing

injectivity using sensing modes with strong low-cost potential (VSP and DAS).

Field data analysis and processing

In January 2022, a rapid-repeat time-lapse VSP seismic experiment (named Tiny bubbles) have been conducted at the CMC Newell County Facility in Alberta, Canada. The rapid-repeat VSP experiment was designed to sense raypaths crossing the CO₂ pressure and fluid plumes, which are positioned in the vicinity of a shallow formation (300m depth). The geometry of the experiment is summarized in Figure 1. The CO₂ entered the Basal Belly River Sandstone (BBRS) formation, forming pressure and fluid plumes between depths of 290-305 m, and the pressure measured at 267 m is shown in Figure 2. The Vibroseis source is 215 m away from the observation well, and the injection well is located between the source and the observation well with 20 m offset from the observation well. The 24 3C geophones are located from 190 m to 305 m with a space interval of 5 m, while the DAS fiber is located from 80 m to 337 m with a space interval of 1 m.

The source was repeatedly activated to densely sample this subsurface volume during twice injections of CO₂. 1281 shots were taken over the 92-hour experiment; these occurred in 64 clusters (Figure 2), with roughly 20 shots taken in rapid succession within each cluster.

To prepare the data for 2D elastic FWI, rotation of 3C geophone VSP data into radial (called Hmax in the paper) and vertical components is required using polarization analysis. Concurrently, depth registration of simultaneously acquired DAS VSP data was carried out, which we addressed using a cross-correlation scanning scheme. The DAS data measure the strain ratio, and thus it was converted to strain by -90° phase shift. Figure 3 shows the vertical component, Hmax component, and DAS data of the baseline data (cluster 1) after preprocessing.

After preprocessing, we analyzed the geophone and DAS data to detect the amplitude normalization differences between the repeated surveys, as indicators of time-lapse fluid changes. Figures 4-6 show the amplitude normalization differences of those selected monitor clusters data (green squares in Figure 2) between the baseline data (cluster 1), where (1) cluster 3 is near cluster 1; (2) cluster 5 is around the beginning of the first CO₂ injection; (3) cluster 13 is during the first CO₂ injection; (4) cluster 22 is

Real-time and quantitative monitoring of CO₂ injection

at the end of the first CO₂ injection; (5) cluster 31 is between the twice CO₂ injection; (6) cluster 39 is around the beginning of the second CO₂ injection; (7) cluster 47 is during the second CO₂ injection. (8) cluster 56 is at the end of the second CO₂ injection;(9) cluster 64 is at the end.

It can be seen that the normalization anomaly appears around 300 m in vertical components and 305 m in horizontal components. The pressure or fluid conditions in cluster 3 and cluster 1 are relatively similar, which means that the anomaly at 305 m in cluster 3 is likely not affected by pressure or fluid injection. As a comparison, the anomaly at 300m occurs after CO₂ injection. Therefore, inversion is necessary to make sure whether the anomaly at 300m is influenced by the pressure and fluid.

We apply the frequency-domain EFWI to the field data, hence, we analyze their amplitude normalization in the frequency domain by 10-25 hz (Figure 5) and 55-65 hz (Figure 6). While lower frequencies are ideal, we have found that 10 Hz is the lowest acceptable frequency for seismic signal-to-noise ratios. After several sets of tests, the result of dividing into these two group frequencies can get better results. The vertical component anomalies at 300 m are almost invisible in Figure 5 (10-25 Hz) but obvious in Figure 6 (55-65 Hz). Therefore, our inversion strategy takes the 55-65hz frequency as the main contribution to obtaining the time-lapse images.

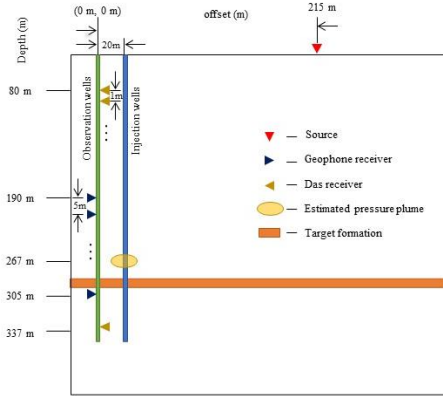


Figure 1. The geometry of Tiny bubbles seismic source, injection, and observation wells.

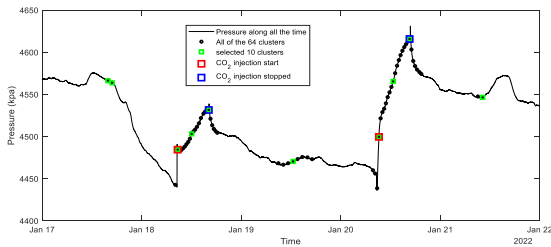


Figure 2. Pressure changes at 267 m (black curve) along the time from Jan 17 to Jan 22, 2022. Black circles are the times at which all 64 monitoring shot clusters occurred. Red squares and blue squares indicate the CO₂ injection and CO₂ stopped, respectively. Green squares are the selected clusters.

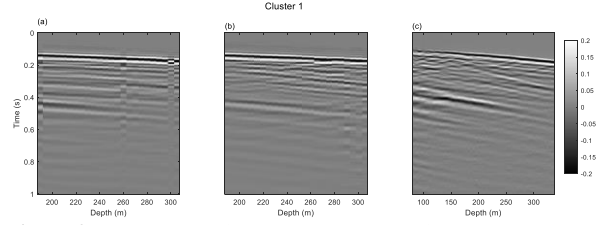


Figure 3. The baseline field data (cluster 1) after preprocessing. (a)-(c) are the geophone vertical component, geophone Hmax component, and DAS data, respectively.

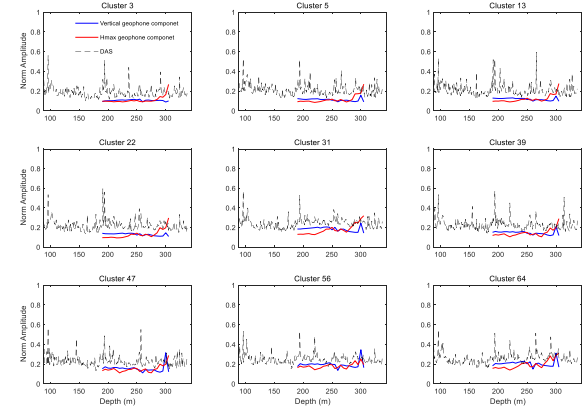


Figure 4. The normalization of difference between monitor data (the selected clusters in Figure 1) and baseline data in the time domain for vertical geophone, Hmax geophone, and DAS data.

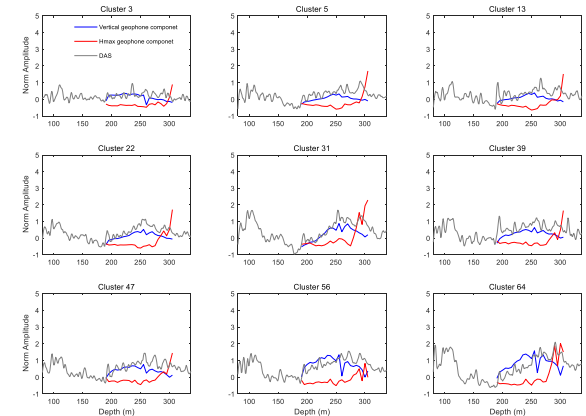


Figure 5. The normalization of difference between monitor data and baseline data with 10-25Hz.

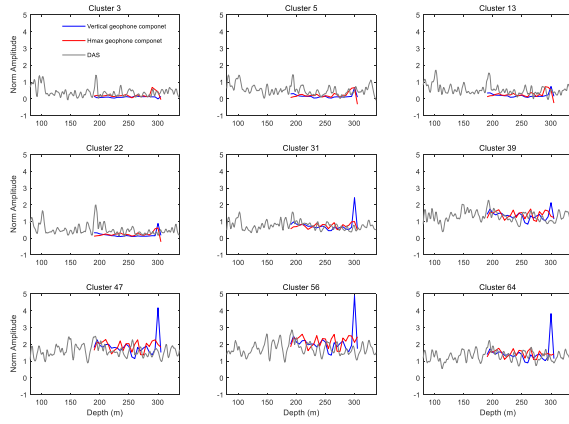


Figure 6. The normalization of difference between monitor data and baseline data with 55-65Hz.

EFWI Method

Here we apply P-velocity (V_p)-parameterized ERTM based on VSP data with a fixed source and raypaths designed to intersect the pressure and injection plumes. The main time-lapse VSP inversion workflow involved EFWI of the combined geophone and DAS data (Eaid et al., 2020), which in turn required the application of methods for effective source estimation (Keating et al., 2021), and implementation of a time-lapse inversion strategy. The inversion was implemented by combining the vertical and Hmax components of the geophone data with the DAS data via the FWI objective function receiver sampling matrix. Second, in the effective source approach, we assume a line source at a depth that generates the wavefield that would be obtained by propagation through the near-surface. We invert for both model parameters and this unknown source. Finally, we use the parallel time-lapse strategy, where monitor and baseline inversions use the same starting model.

The inversion approach could be divided into three steps: first is the source-only inversion based on baseline data and second is model-only inversion from 10 Hz to 25 Hz for baseline data, and final is the model-only inversion from 55 Hz to 65 Hz for all of the 64 clusters data. Based on the strategy, monitor data inversions and baseline data inversion use the same effective source and low-frequency inverted models. The model-only inversion between 10 Hz and 25 Hz applies the combined DAS and geophone data, while the model-only inversion between 55 Hz and 65 Hz only uses the geophone data for that the anomaly at 300m occurs in the geophone vertical component instead of the DAS data.

Inversion for field data

The model size is 240 m in the x -direction and 350 m in the z -direction, and the space interval is 2.5 m. In this report, we consider five frequency bands for the inversion, each consisting of 12 frequencies, starting with the lowest frequencies and ending with a band spanning from low to high frequencies. We consider an effective source depth of 40 m to implement the effective sources inversion strategy.

Figure 7 shows the initial and inverted models of V_p , S-velocity (V_s), and density (ρ) for baseline data. Figure 8 shows the comparison of the inverted V_p , V_s , and ρ models with the well logs data, which indicates that the inverted model has a relatively good consistent trend with log data. Figure 9 indicates the snapshots of inverted time-lapse V_p models which include the injection well (red line), the injection depth (rose red dash line), injection hours, and the amount of CO₂ injection. The time-lapse anomaly (V_p) is different from the noise and the time-lapse anomaly located at 300 m (injection location), which have a good consistency with the field data normalization in Figure 6. We extract the inversion time-lapse V_p value located ($x = 5$ m, $z = 300$ m) for all 64 clusters (shown in Figure 10). The FWI images track the real effects of pressure or fluid injection:

- It can be seen that the overall trend of time-lapse anomaly (V_p , V_s , and ρ) keeps decreasing with CO₂ injection (from cluster 1 to cluster 64).
- During the first CO₂ injection, the time-lapse anomaly has not indicated significant changes, because the amount of CO₂-containing fluid migrating to the observation wells is insufficient to cause significant changes in time-lapse V_p , V_s and ρ (from cluster 5 to cluster 22).
- Based on the continuous migration of fluid, the time-lapse anomaly decreases after a period of time of the pressure and CO₂ injection stopped (from cluster 23 to cluster 38).
- During the second CO₂ injection, the time-lapse anomaly drops significantly in a short time, which is due to the influence of fluid and pressure. Because CO₂ migrating to the observation well continued to increase, and the wellhead pressure increment was larger compared with the first CO₂ injection (from cluster 39 to cluster 56).
- After the second CO₂ injection stops, the time-lapse anomaly also rises to a certain extent as the pressure releases to the initial state. Because the CO₂-containing fluid in the vicinity of the observation well has already changed compared with the baseline cluster data, the time-lapse V_p , V_s and ρ cannot be increased to the original state (from cluster 57 to cluster 64).

Real-time and quantitative monitoring of CO₂ injection

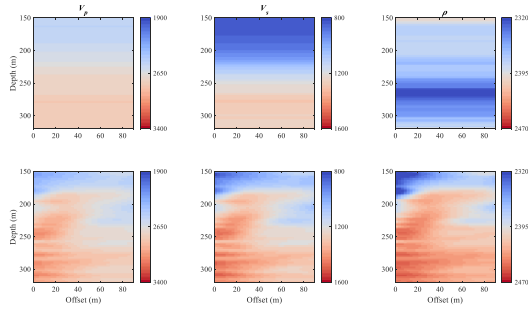


Figure 7. Initial (upper) and inverted (down) models of V_p , V_s , and ρ for baseline data (cluster 1).

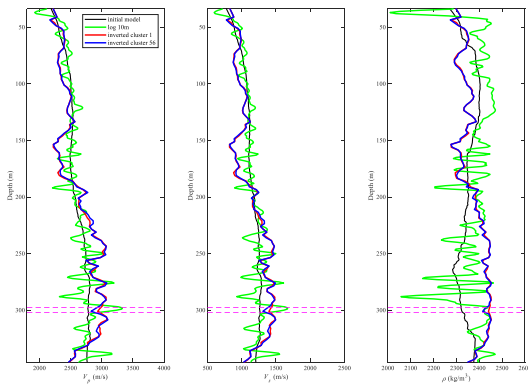


Figure 8. The comparison of the initial and inverted velocities models with the well logs data.

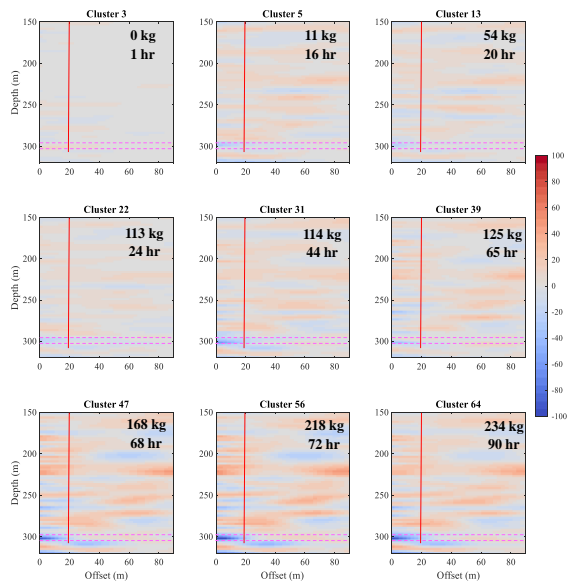


Figure 9. The inverted time-lapse V_p models.

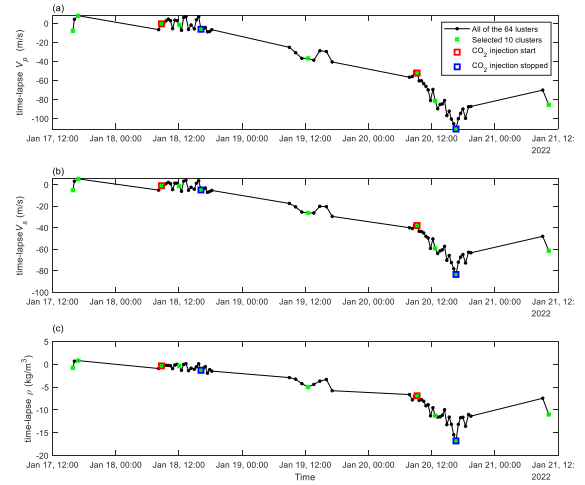


Figure 10. The time-lapse V_p , V_s , and ρ models for all clusters.

Conclusion

These clusters' FWI images indicate the dynamic changes of V_p , V_s , and ρ , and track the real effects of pressure or fluid injection. The time-lapse anomaly (V_p , V_s , and ρ) keeps decreasing with the increase of CO₂ injection or pressure. When the pressure is decreased to the initial pressure, the time-lapse anomaly will increase accordingly but does not reach the initial stage because of the existence of fluid. In addition, the ERTM results indicate that the VSP-DAS included in sparse-space geophone data is a reasonable and practical monitoring mode.

Acknowledgments

This work was funded by CREWES industrial sponsors and NSERC (Natural Science and Engineering Research Council of Canada) through the grant CRDPJ 543578-19. The data were acquired through a collaboration with the Containment and Monitoring Institute, Carbon Management Canada.